International Tables for Crystallography (2006). Vol. C, Section 4.4.2.4, pp. 435–438.

eter, first conceived by Brockhouse (1958). A pulse of monochromatic neutrons is obtained when the reciprocal-lattice vector of a rotating crystal bisects the angle between two collimators. Effectively, the neutron **k** vector is changed in both direction and magnitude, depending on whether the crystal is moving towards or away from the neutron. For the rotating crystal, both of these situations occur simultaneously for different halves of the crystal, so that the net effect over the beam cross section is that a wider energy band is reflected than from the crystal at rest, and that, depending on the sense of rotation, the beam is either focused or defocused in time (Meister & Weckerman, 1972).

The Bragg reflection of neutrons from a crystal moving parallel to its lattice planes is illustrated in Fig. 4.4.2.3(*b*). It can be seen that the moving crystal selects a larger Δk than the crystal at rest, so that the reflected intensity is higher. Furthermore, it is possible under certain conditions to orientate the diffracted phase-space volume orthogonal to the diffraction vector. In this way, a monochromatic divergent beam can be obtained from a collimated beam with a larger energy spread. This provides an elegant means of producing a divergent beam with a sufficiently wide momentum spread to be scanned by the Doppler crystal of a backscattering instrument (Schelten & Alefeld, 1984).

Finally, an alternative method of scanning the energy of a monochromator in backscattering is to apply a steady but uniform temperature variation. The monochromator crystal must have a reasonable thermal expansion coefficient, and care has to be taken to ensure a uniform temperature across the crystal.

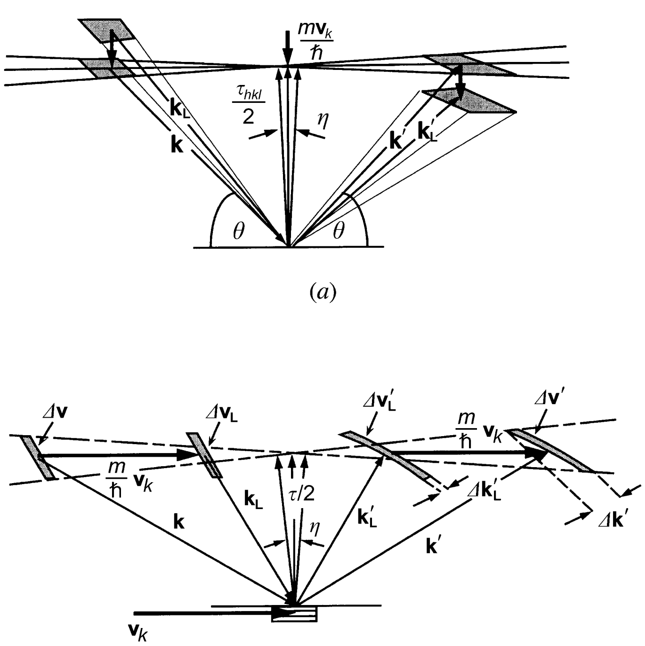

Fig. 4.4.2.3. Momentum-space representation of Bragg scattering from a crystal moving (*a*) perpendicular and (*b*) parallel to the diffracting planes with a velocity $\mathbf{v}_k$. The vectors $\mathbf{k}_L$ and $\mathbf{k}'_L$ refer to the incident and reflected wavevectors in the laboratory frame of reference. In (*a*), depending on the direction of $\mathbf{v}_k$, the reflected wavevector is larger or smaller than the incident wavevector, $\mathbf{k}_L$. In (*b*), a larger incident reciprocal-space volume, $\Delta\mathbf{v}_L$, is selected by the moving crystal than would have been selected by the crystal at rest. The reflected reciprocal-space element, $\Delta\mathbf{v}'_L$, has a large divergence, but can be arranged to be normal to $\mathbf{k}'_L$, hence improving the resolution $\Delta\mathbf{k}'_L$.

Table 4.4.2.2. *Neutron scattering-length densities, Nb_{coh}, for some commonly used materials*

Material	Nb (10^{-6} Å^{-2})
^{58}Ni	13.31
Diamond	11.71
Nickel	9.40
Quartz	3.64
Germanium	3.62
Silver	3.50
Aluminium	2.08
Silicon	2.08
Vanadium	−0.27
Titanium	−1.95
Manganese	−2.95

4.4.2.4. *Mirror reflection devices*

The refractive index, n, for neutrons of wavelength λ propagating in a nonmagnetic material of atomic density N is given by the expression

$$n^2 = 1 - \frac{\lambda^2 Nb_{\rm coh}}{\pi}, \qquad (4.4.2.4)$$

where $b_{\rm coh}$ is the mean coherent scattering length. Values of the scattering-length density $Nb_{\rm coh}$ for some common materials are listed in Table 4.4.2.2, from which it can be seen that the refractive index for most materials is slightly less than unity, so that total external reflection can take place. Thus, neutrons can be reflected from a smooth surface, but the critical angle of reflection, γ_c, given by

$$\gamma_c = \lambda \sqrt{\frac{Nb_{\rm coh}}{\pi}}, \qquad (4.4.2.5)$$

is small, so that reflection can only take place at grazing incidence. The critical angle for nickel, for example, is 0.1° Å^{-1}.

Because of the shallowness of the critical angle, reflective optics are traditionally bulky, and focusing devices tend to have long focal lengths. In some cases, however, depending on the beam divergence, a long mirror can be replaced by an equivalent stack of shorter mirrors.

4.4.2.4.1. *Neutron guides*

The principle of mirror reflection is the basis of neutron guides, which are used to transmit neutron beams to instruments that may be situated up to 100 m away from the source (Christ & Springer, 1962; Maier-Leibnitz & Springer, 1963). A standard neutron guide is constructed from boron glass plates assembled to form a rectangular tube, the dimensions of which may be up to 200 mm high by 50 mm wide. The inner surface of the guide is coated with approximately 1200 Å of either nickel, ^{58}Ni ($\gamma_c = 0.12^\circ$ Å^{-1}), or a 'supermirror' (described below). The guide is usually evacuated to reduce losses due to absorption and scattering of neutrons in air.

Theoretically, a neutron guide that is fully illuminated by the source will transmit a beam with a square divergence of full width $2\gamma_c$ in both the horizontal and vertical directions, so that the transmitted solid angle is proportional to λ^2. In practice, owing to imperfections in the assembly of the guide system, the divergence profile is closer to Gaussian than square at the end of a long guide. Since the neutrons may undergo a large number of reflections in the guide, it is important to achieve a high reflectivity. The specular reflectivity is determined by the surface roughness, and typically values in the range 98.5 to 99% are achieved. Further transmission losses occur due to imperfections in the alignment of the sections that make up the guide.

The great advantage of neutron guides, in addition to the transport of neutrons to areas of low background, is that they can be multiplexed, *i.e.* one guide can serve many instruments. This is achieved either by deflecting only a part of the total cross section to a given instrument or by selecting a small wavelength range from the guide spectrum. In the latter case, the selection device (usually a crystal monochromator) must have a high transmission at other wavelengths.

If the neutron guide is curved, the transmission becomes wavelength dependent, as illustrated in Fig. 4.4.2.4. In this case, one can define a characteristic wavelength, λ^*, given by the relation $\theta^* = \sqrt{2a/\rho}$, so that

$$\lambda^* = \sqrt{\frac{\pi}{Nb_{\rm coh}}}\sqrt{\frac{2a}{\rho}} \qquad (4.4.2.6)$$

(where a is the guide width and ρ the radius of curvature), for which the theoretical transmission drops to 67%. For wavelengths less than λ^*, neutrons can only be transmitted by 'garland' reflections along the concave wall of the curved guide. Thus, the guide acts as a low-pass energy filter as long as its length is longer than the direct line-of-sight length $L_1 = \sqrt{8a\rho}$. For example, a 3 cm wide nickel-coated guide whose characteristic wavelength is 4 Å (radius of curvature 1300 m) must be at least 18 m long to act as a filter. The line-of-sight length can be reduced by subdividing the guide into a number of narrower channels, each of which acts as a miniguide. The resulting device, often referred to as a neutron bender, since deviation of the beam is achieved more rapidly, is used in beam deviators (Alefeld *et al.*, 1988) or polarizers (Hayter, Penfold & Williams, 1978). A microbender was devised by Marx (1971) in which the channels were made by evaporating alternate layers of aluminium (transmission layer) and nickel (mirror layer) onto a flexible smooth substrate.

Tapered guides can be used to reduce the beam size in one or two dimensions (Rossbach *et al.*, 1988), although, since mirror reflection obeys Liouville's theorem, focusing in real space is achieved at the expense of an increase in divergence. This fact can be used to calculate analytically the expected gain in neutron flux at the end of a tapered guide (Anderson, 1988). Alternatively, focusing can be achieved in one dimension using a bender in which the individual channel lengths are adjusted to create a focus (Freund & Forsyth, 1979).

4.4.2.4.2. *Focusing mirrors*

Optical imaging of neutrons can be achieved using ellipsoidal or torroidal mirrors, but, owing to the small critical angle of reflection, the dimensions of the mirrors themselves and the radii of curvature must be large. For example, a 4 m long toroidal mirror has been installed at the IN15 neutron spin echo spectrometer at the Institut Laue–Langevin, Grenoble (Hayes *et al.*, 1996), to focus neutrons with wavelengths greater than 15Å. The mirror has an in-plane radius of curvature of 408.75 m, and the sagittal radius is 280 mm. A coating of ^{65}Cu is used to obtain a high critical angle of reflection while maintaining a low surface roughness. Slope errors of less than 2.5×10^{-5} rad (r.m.s.) combined with a surface roughness of less than 3Å allow a minimum resolvable scattering vector of about 5×10^{-4} Å^{-1} to be reached.

For best results, the slope errors and the surface roughness must be low, in particular in small-angle scattering applications, since diffuse scattering from surface roughness gives rise to a halo around the image point. Owing to its low thermal expansion coefficient, highly polished Zerodur is often chosen as substrate.

4.4.2.4.3. *Multilayers*

Schoenborn, Caspar & Kammerer (1974) first pointed out that multibilayers, comprising alternating thin films of different scattering-length densities ($Nb_{\rm coh}$) act like two-dimensional crystals with a d spacing given by the bilayer period. With modern deposition techniques (usually sputtering), uniform films of thickness ranging from about twenty to a few hundred ångströms can be deposited over large surface areas of the order of 1 m^2. Owing to the rather large d spacings involved, the Bragg reflection from multilayers is generally at grazing incidence, so that long devices are required to cover a typical beam width, or a stacked device must be used. However, with judicious choice of the scattering-length contrast, the surface and interface roughness, and the number of layers, reflectivities close to 100% can be reached.

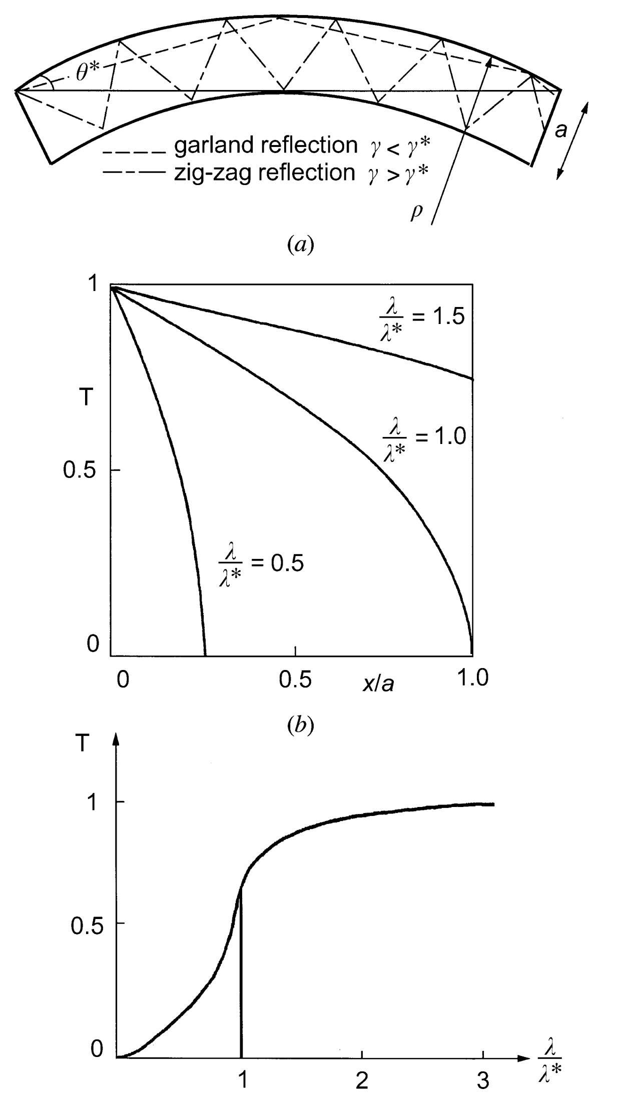

Fig. 4.4.2.4. In a curved neutron guide, the transmission becomes λ dependent: (*a*) the possible types of reflection (garland and zig-zag), the direct line-of-sight length, the critical angle θ^*, which is related to the characteristic wavelength $\lambda^* = \theta^*\sqrt{\pi/Nb_{\rm coh}}$; (*b*) transmission across the exit of the guide for different wavelengths, normalized to unity at the outside edge; (*c*) total transmission of the guide as a function of λ.

Fig. 4.4.2.5 illustrates how variation in the bilayer period can be used to produce a monochromator (the minimum $\Delta\lambda/\lambda$ that can be achieved is of the order of 0.5%), a broad-band device, or a 'supermirror', so called because it is composed of a particular sequence of bilayer thicknesses that in effect extends the region of total mirror reflection beyond the ordinary critical angle (Turchin, 1967; Mezei, 1976; Hayter & Mook, 1989). Supermirrors have been produced that extend the critical angle of nickel by a factor, m, of between three and four with reflectivities better than 90%. Such high reflectivities enable supermirror neutron guides to be constructed with flux gains, compared with nickel guides, close to the theoretical value of m^2.

The choice of the layer pairs depends on the application. For non-polarizing supermirrors and broad-band devices (Høghøj, Anderson, Ebisawa & Takeda, 1996), the Ni/Ti pair is commonly used, either pure or with some additions to relieve strain and stabilize interfaces (Elsenhans *et al.*, 1994) or alter the magnetism (Anderson & Høghøj, 1996), owing to the high contrast in scattering density, while for narrow-band monochromators a low contrast pair such as W/Si is more suitable.

4.4.2.4.4. *Capillary optics*

Capillary neutron optics, in which hollow glass capillaries act as waveguides, are also based on the concept of total external reflection of neutrons from a smooth surface. The advantage of capillaries, compared with neutron guides, is that the channel sizes are of the order of a few tens of micrometres, so that the radius of curvature can be significantly decreased for a given characteristic wavelength [see equation (4.4.2.6)]. Thus, neutrons can be efficiently deflected through large angles, and the device can be more compact.

Two basic types of capillary optics exist, and the choice depends on the beam characteristics required. Polycapillary fibres are manufactured from hollow glass tubes several centimetres in diameter, which are heated, fused and drawn multiple times until bundles of thousands of micrometre-sized channels are formed having an open area of up to 70% of the cross section. Fibre outer diameters range from 300 to 600 µm and contain hundreds or thousands of individual channels with inner diameters between 3 and 50 µm. The channel cross section is usually hexagonal, though square channels have been produced, and the inner channel wall surface roughness is typically less than 10 Å r.m.s., giving rise to very high reflectivities. The principal limitations on transmission efficiency are the open area, the acceptable divergence (note that the critical angle for glass is 1 mrad Å $^{-1}$) and reflection losses due to absorption and scattering. A typical optical device will comprise hundreds or thousands of fibres threaded through thin screens to produce the required shape.

Fig. 4.4.2.6 shows typical applications of polycapillary devices. In Fig. 4.4.2.6(*a*), a polycapillary lens is used to refocus neutrons collected from a divergent source. The half lens depicted in Fig. 4.4.2.6(*b*) can be used either to produce a nearly parallel (divergence = $2\gamma_c$) beam from a divergent source or (in the reverse sense) to focus a nearly parallel beam, *e.g.* from a neutron guide. The size of the focal point depends on the channel size, the beam divergence, and the focal length of the lens. For example, a polycapillary lens used in a prompt γ-activation analysis instrument at the National Institute of Standards and Technology to focus a cold neutron beam from a neutron guide results in a current density gain of 80 averaged over the focused beam size of 0.53 mm (Chen *et al.*, 1995).

Fig. 4.4.2.6(*c*) shows another simple application of polycapillaries as a compact beam bender. In this case, such a bender may be more compact than an equivalent multichannel guide bender, although the accepted divergence will be less. Furthermore, as with curved neutron guides, owing to the wavelength dependence of the critical angle the capillary curvature can be used to filter out thermal or high-energy neutrons.

It should be emphasized that the applications depicted in Fig. 4.4.2.6 obey Liouville's theorem, in that the density of neutrons in phase space is not changed, but the shape of the phase-space volume is altered to meet the requirements of the experiment,

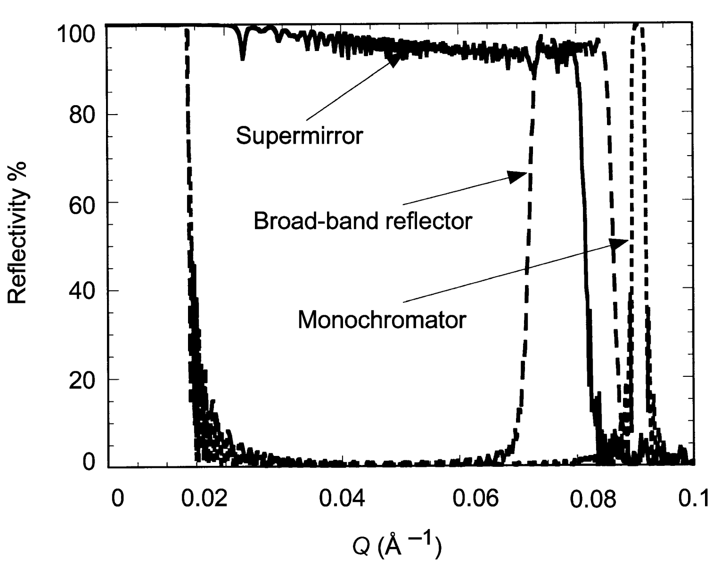

Fig. 4.4.2.5. Illustration of how a variation in the bilayer period can be used to produce a monochromator, a broad-band device, or a supermirror.

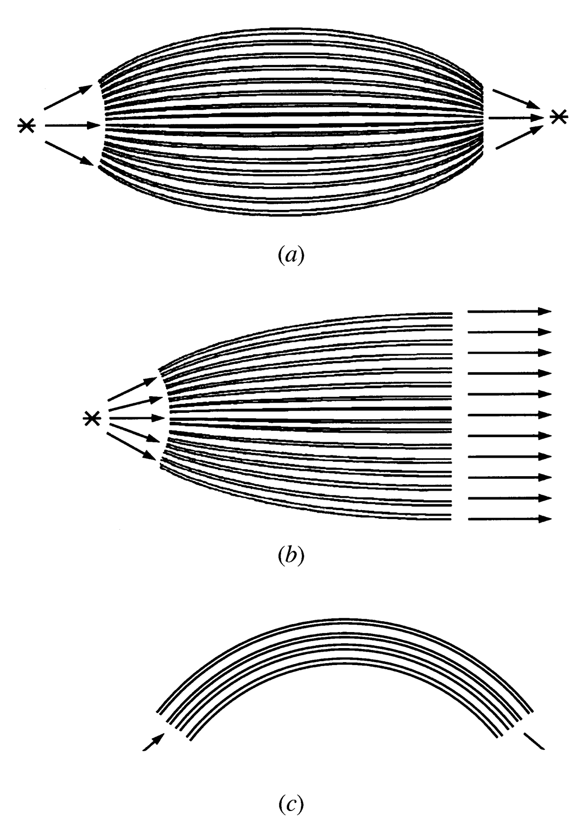

Fig. 4.4.2.6. Typical applications of polycapillary devices: (*a*) lens used to refocus a divergent beam; (*b*) half-lens to produce a nearly parallel beam or to focus a nearly parallel beam; (*c*) a compact bender.

i.e. there is a simple trade off between beam dimension and divergence.

The second type of capillary optic is a monolithic configuration. The individual capillaries in monolithic optics are tapered and fused together, so that no external frame assembly is necessary (Chen-Mayer *et al.*, 1996). Unlike the multifibre devices, the inner diameters of the channels that make up the monolithic optics vary along the length of the component, resulting in a smaller more compact design.

Further applications of capillary optics include small-angle scattering (Mildner, 1994) and lenses for high-spatial-resolution area detection.

4.4.2.5. *Filters*

Neutron filters are used to remove unwanted radiation from the beam while maintaining as high a transmission as possible for the neutrons of the required energy. Two major applications can be identified: removal of fast neutrons and γ-rays from the primary beam and reduction of higher-order contributions (λ/n) in the secondary beam reflected from crystal monochromators. In this section, we deal with non-polarizing filters, *i.e.* those whose transmission and removal cross sections are independent of the neutron spin. Polarizing filters are discussed in the section concerning polarizers.

Filters rely on a strong variation of the neutron cross section with energy, usually either the wavelength-dependent scattering cross section of polycrystals or a resonant absorption cross section. Following Freund (1983), the total cross section determining the attenuation of neutrons by a crystalline solid can be written as a sum of three terms,

$$\sigma = \sigma_{\rm abs} + \sigma_{\rm tds} + \sigma_{\rm Bragg}. \qquad (4.4.2.7)$$

Here, $\sigma_{\rm abs}$ is the true absorption cross section, which, at low energy, away from resonances, is proportional to $E^{-1/2}$. The temperature-dependent thermal diffuse cross section, $\sigma_{\rm tds}$, describing the attenuation due to inelastic processes, can be split into two parts depending on the neutron energy. At low energy, $E \ll k_b\Theta_D$, where k_b is Boltzmann's constant and Θ_D is the characteristic Debye temperature, single-phonon processes dominate, giving rise to a cross section, $\sigma_{\rm sph}$, which is also proportional to $E^{-1/2}$. The single-phonon cross section is proportional to $T^{7/2}$ at low temperatures and to T at higher temperatures. At higher energies, $E \geq k_b\Theta_D$, multiphonon and multiple-scattering processes come into play, leading to a cross section, $\sigma_{\rm mph}$, that increases with energy and temperature. The third contribution, $\sigma_{\rm Bragg}$, arises due to Bragg scattering in single- or polycrystalline material. At low energies, below the Bragg cut-off ($\lambda > 2d_{\rm max}$), $\sigma_{\rm Bragg}$ is zero. In polycrystalline materials, the cross section rises steeply above the Bragg cut-off and oscillates with increasing energy as more reflections come into play. At still higher energies, $\sigma_{\rm Bragg}$ decreases to zero.

In single-crystalline material above the Bragg cut-off, $\sigma_{\rm Bragg}$ is characterized by a discrete spectrum of peaks whose heights and widths depend on the beam collimation, energy resolution, and the perfection and orientation of the crystal. Hence a monocrystalline filter has to be tuned by careful orientation.

The resulting attenuation cross section for beryllium is shown in Fig. 4.4.2.7. Cooled polycrystalline beryllium is frequently used as a filter for neutrons with energies less than 5 meV, since there is an increase of nearly two orders of magnitude in the attenuation cross section for higher energies. BeO, with a Bragg cut-off at approximately 4 meV, is also commonly used.

Pyrolytic graphite, being a layered material with good crystalline properties along the c direction but random orientation perpendicular to it, lies somewhere between a polycrystal and a single crystal as far as its attenuation cross section is concerned. The energy-dependent cross section for a neutron beam incident along the c axis of a pyrolytic graphite filter is shown in Fig. 4.4.2.8, where the attenuation peaks due to the 00ξ reflections can be seen. Pyrolytic graphite serves as an efficient second- or third-order filter (Shapiro & Chesser, 1972) and can be 'tuned' by slight misorientation away from the c axis.

Further examples of typical filter materials (*e.g.* silicon, lead, bismuth, sapphire) can be found in the paper by Freund (1983).

Resonant absorption filters show a large increase in their attenuation cross sections at the resonant energy and are therefore used as selective filters for that energy. A list of typical filter materials and their resonance energies is given in Table 4.4.2.3.

4.4.2.6. *Polarizers*

Methods used to polarize a neutron beam are many and varied, and the choice of the best technique depends on the instrument and the experiment to be performed. The main parameter that has to be considered when describing the effectiveness of a given polarizer is the polarizing efficiency, defined as

$$P = (N_+ - N_-)/(N_+ + N_-), \qquad (4.4.2.8)$$

where N_+ and N_- are the numbers of neutrons with spin parallel (+) or antiparallel (−) to the guide field in the outgoing beam. The second important factor, the transmission of the wanted spin state, depends on various factors, such as acceptance angles, reflection, and absorption.

4.4.2.6.1. *Single-crystal polarizers*

The principle by which ferromagnetic single crystals are used to polarize and monochromate a neutron beam simultaneously is shown in Fig. 4.4.2.9. A field **B**, applied perpendicular to the scattering vector $\boldsymbol{\kappa}$, saturates the atomic moments $\mathbf{M}_\nu$ along the field direction. The cross section for Bragg reflection in this geometry is

$$({\rm d}\sigma/{\rm d}\Omega) = F_N(\boldsymbol{\kappa})^2 + 2F_N(\boldsymbol{\kappa})F_M(\boldsymbol{\kappa})(\mathbf{P}\cdot\boldsymbol{\mu}) + F_M(\boldsymbol{\kappa})^2, \quad (4.4.2.9)$$

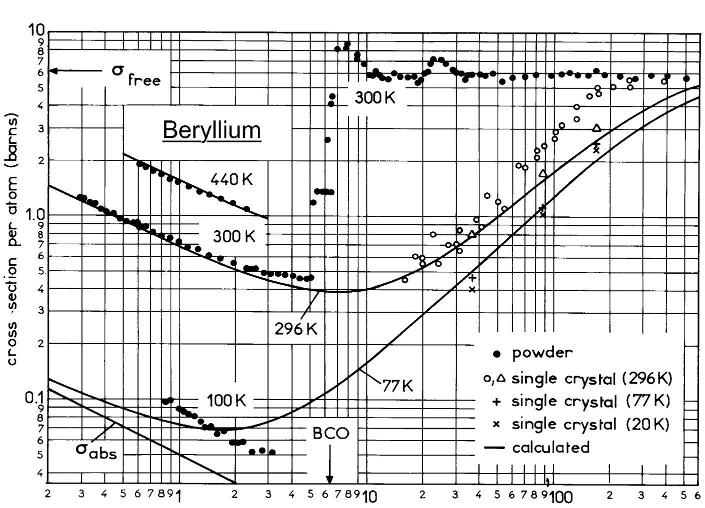

Fig. 4.4.2.7. Total cross section for beryllium in the energy range where it can be used as a filter for neutrons with energy below 5 meV (Freund, 1983).

references